PHYSICAL REVIEW D **93,** 054003 (2016)

$\Lambda_b \to (\Lambda_c, p)\tau\nu$ decays within standard model and beyond

Rupak Dutta*

National Institute of Technology Silchar, Silchar 788010, India

(Received 18 December 2015; published 2 March 2016)

Deviations from the standard model prediction have been observed in several leptonic and semileptonic B meson decays to $\tau\nu$ final states mediated via $b \to u$ and $b \to c$ charged current interactions. The measured value of the ratio of branching ratios R_π^l of $B^- \to \tau^-\nu_\tau$ to $B^0 \to \pi^+ l^-\nu$ decays, where $l = (e, \mu)$, is larger than the standard model prediction by more than a factor of 2. Similarly, a combined excess of 3.9σ from the standard model expectation has been reported by HFAG for the values of R_D and R_{D^*}, where R_{D,D^*} represents the ratio of branching ratios of $B \to (D, D^*)\tau\nu$ to corresponding $B \to (D, D^*)l\nu$ decays, respectively. Very recently, a hint of lepton flavor violation has been observed in the ratio of branching fractions of $B \to Ke^+e^-$ to $B \to K\mu^+\mu^-$ decays as well. In this context, we employ an effective Lagrangian approach to study the decay branching fractions and the ratio of branching fractions of $\Lambda_b \to \Lambda_c l\nu$ and $\Lambda_b \to pl\nu$ decays within the standard model and beyond. We constrain the new physics parameter space using the existing experimental data on R_D, R_{D^*}, and R_π^l. We give predictions for various observables in the context of various new physics scenarios.

DOI: 10.1103/PhysRevD.93.054003

I. INTRODUCTION

Hints of lepton flavor violation have been observed in various leptonic and semileptonic B decays. Recently, the LHCb Collaboration [1] has measured the ratio of branching fractions of $B \to Ke^+e^-$ to $B \to K\mu^+\mu^-$ decays to be $R_K^{\mu e} = 0.745^{+0.090}_{-0.074}$ in the dilepton invariant mass squared range $(1 < q^2 < 6)$ GeV^2. It differs from the standard model (SM) expectation at the 2.6σ significance level. Similar tensions between theory and experiment have been observed in $B \to \tau\nu$ and $B \to (D, D^*)\tau\nu$ decays mediated via $b \to u$ and $b \to c$ charged current interactions as well [2–5]. A combined excess of 3.9σ from the SM prediction has been reported by HFAG on R_D and R_{D^*}, where

$$R_D = \frac{\mathcal{B}(\bar{B}^0 \to D\tau\nu)}{\mathcal{B}(\bar{B}^0 \to Dl\nu)} = 0.391 \pm 0.041 \pm 0.028,$$
$$R_{D^*} = \frac{\mathcal{B}(\bar{B}^0 \to D^*\tau\nu)}{\mathcal{B}(\bar{B}^0 \to D^*l\nu)} = 0.322 \pm 0.018 \pm 0.012. \quad (1)$$

Again, there is a discrepancy of more than 2σ with the SM expectation in the measured ratio $R_\pi^l = 0.73 \pm 0.15$ [6],

$$R_\pi^l = \frac{\tau_{B^0}}{\tau_{B^-}} \frac{\mathcal{B}(B^- \to \tau^-\nu_\tau)}{\mathcal{B}(B^0 \to \pi^+ l^-\nu_l)}, \quad (2)$$

where l represents either an electron or a muon, respectively. The recent value of $\mathcal{B}(B^- \to \tau^-\nu_\tau) = (11.4 \pm 2.2) \times 10^{-5}$ [7–9] is slightly larger than the SM expectation [10–12]. Again, the most recent result of $\mathcal{B}(B^- \to \tau^-\nu_\tau) = (12.5 \pm 2.8 \pm 2.7) \times 10^{-5}$ reported by Belle [13] is consistent with their earlier result. Moreover, the measured value of $\mathcal{B}(B^0 \to \pi^+ l^-\nu_l) = (14.6 \pm 0.7) \times 10^{-5}$ [14–16] is consistent with the SM prediction. The Belle experiment recently reported an upper limit on the total rate $\mathcal{B}(B^0 \to \pi^-\tau\nu) < 2.5 \times 10^{-4}$ [17] which is close to the SM prediction [18]. A prediction on the ratio of branching ratios R_π of $B \to \pi\tau\nu$ to the corresponding $B \to \pi l\nu$ decays has also been reported in Refs. [18–22]. Several phenomenological works have been done in order to explain the discrepancies in R_D, R_{D^*}, R_π^l, and $R_K^{\mu e}$; see, in particular, Refs. [6,19,21,23–50]. The ratio of branching ratios such as R_D, R_{D^*}, R_π^l, R_π, and $R_K^{\mu e}$ are excellent observables to test for new physics (NP) for two main reasons. First, these ratios of branching ratios are independent of the CKM matrix element and hence the uncertainties associated with the CKM matrix elements do not enter into these ratios. Second, uncertainties associated with the hadronic form factors are also reduced while taking these ratios.

Precise determination of the CKM matrix elements $|V_{cb}|$ and $|V_{ub}|$ is interesting in itself as there are tensions between exclusive and inclusive determination of $|V_{cb}|$ and $|V_{ub}|$ from semileptonic B decays. The typical relative accuracy is about 2% for $|V_{cb}|$; however, the precision on $|V_{ub}|$ is not better than 12% [51]. The magnitude $|V_{ub}|$ can be measured via semileptonic $b \to u$ transition decays. The world average using the exclusive $b \to u$ transition decay channels $\bar{B}^0 \to \pi^+ l\nu$ and $B^- \to \pi^0 l\nu$ is $|V_{ub}| = (32.8 \pm 2.9) \times 10^{-4}$ [52]. Very recently, LHCb has measured the ratio of partially integrated rates of baryonic $b \to u$ and $b \to c$ decays $\Lambda_b \to p\mu\nu$ and $\Lambda_b \to \Lambda_c\mu\nu$ and put constraints on the ratio of $|V_{ub}|$ and $|V_{cb}|$. Combined with the theoretical calculations and previously measured value of $|V_{cb}| = (39.5 \pm 0.8) \times 10^{-3}$ [9], the obtained value of

*rupak@phy.nits.ac.in

$|V_{ub}| = (32.7 \pm 2.3) \times 10^{-4}$ [53,54] is in good agreement with the exclusively measured world average. However, it disagrees with the inclusive measurement at a 3.5σ significance level. This is the first measurement of $|V_{ub}|$ using baryonic decay channels. The baryonic $\Lambda_b \to p\mu\nu$ decays mediated via $b \to u$ charge current interactions was not considered before as Λ_b baryons are not produced in the e^+e^- B factory. However, at the LHC, production of the Λ_b baryon is remarkably high—around 20% of the total b hadrons produced [55,56].

The $\Lambda_b \to \Lambda_c \tau\nu$ decay mode has been studied by various authors [57–60]. In Ref. [58], a prediction for the decay branching fractions and the ratio of branching fractions has been presented in the context of SM and various NP couplings. In Ref. [59], a covariant confined quark model has been used to provide the SM prediction on various observables such as total rate, the differential decay distribution, the longitudinal and transverse polarization of the daughter baryon Λ_c and the τ lepton, and the lepton side forward-backward asymmetries. Again, in Ref. [60], a precise calculation of the $\Lambda_b \to \Lambda_c$ and $\Lambda_b \to p$ form factors using lattice QCD with $2+1$ dynamical flavors has been done and the SM prediction of the differential and integrated decay rates of $\Lambda_b \to \Lambda_c l\nu$ and $\Lambda_b \to p l\nu$ decays have been reported. Similarly, in Ref. [61], SM prediction of the decay width and asymmetry parameter for the heavy-to-light semileptonic decays of the Λ_b baryon $\Lambda_b \to p l\nu$ is presented in the covariant confined quark model framework. In this paper, we use the most general effective Lagrangian in the presence of NP and study the effect of various NP couplings on different observables such as differential decay distribution, ratio of branching ratios, forward-backward asymmetries, and the convexity parameter for $\Lambda_b \to \Lambda_c l\nu$ and $\Lambda_b \to p l\nu$ decays in a model-independent way. Although we adopt the same approach, our treatment differs significantly from Ref. [58]. We treat $b \to u$ and $b \to c$ semileptonic decays together in the same framework and perform a combined analysis using the constraints coming from R_D, R_{D^*}, and R_π^l to the end in determining the possible ranges in each observables. Again, for the $\Lambda_b \to \Lambda_c$ and $\Lambda_b \to p$ transition form factors, we use the most precise lattice calculations of Ref. [60].

This paper is organized as follows. In Sec. II, we start with the most general expression for the effective Lagrangian for the $b \to (c,u) l\nu$ transition decays in the presence of NP. A brief discussion on $\Lambda_b \to \Lambda_c$ and $\Lambda_b \to p$ transition form factors is also presented. All the relevant formulas pertinent for our numerical calculation are reported in Sec. II. We define several observables such as differential branching ratio, ratio of branching ratios, forward-backward asymmetries, and convexity parameters for the $\Lambda_b \to \Lambda_c \tau\nu$ and $\Lambda_b \to p\tau\nu$ decay modes. In Sec. III, we start with various input parameters that are used for our analysis. The SM prediction and the effect of various NP couplings on all the observables for the $\Lambda_b \to \Lambda_c \tau\nu$ and $\Lambda_b \to p\tau\nu$ decay modes are presented in Sec. III. We present a brief summary of our results and conclude in Sec. IV.

II. EFFECTIVE LAGRANGIAN AND HELICITY AMPLITUDES

In the presence of NP, the effective weak Lagrangian for the $b \to q' l\nu$ transition decays, where q' is either a u quark or a c quark, can be written as [62,63]

$$\begin{aligned}\mathcal{L}_{\rm eff} = -\frac{4G_F}{\sqrt{2}} V_{q'b}\{&(1+V_L)\bar{l}_L\gamma_\mu\nu_L\bar{q'}_L\gamma^\mu b_L + V_R\bar{l}_L\gamma_\mu\nu_L\bar{q'}_R\gamma^\mu b_R + \tilde{V}_L\bar{l}_R\gamma_\mu\nu_R\bar{q'}_L\gamma^\mu b_L + \tilde{V}_R\bar{l}_R\gamma_\mu\nu_R\bar{q'}_R\gamma^\mu b_R \\ &+ S_L\bar{l}_R\nu_L\bar{q'}_R b_L + S_R\bar{l}_R\nu_L\bar{q'}_L b_R + \tilde{S}_L\bar{l}_L\nu_R\bar{q'}_R b_L + \tilde{S}_R\bar{l}_L\nu_R\bar{q'}_L b_R \\ &+ T_L\bar{l}_R\sigma_{\mu\nu}\nu_L\bar{q'}_R\sigma^{\mu\nu} b_L + \tilde{T}_L\bar{l}_L\sigma_{\mu\nu}\nu_R\bar{q'}_L\sigma^{\mu\nu} b_R\} + \text{H.c.},\end{aligned} \tag{3}$$

where G_F is the Fermi constant, $V_{q'b}$ is the relevant CKM matrix element, and $(q', b, l, \nu)_{R,L} = (\frac{1\pm\gamma_5}{2})(q', b, l, \nu)$. The NP couplings, associated with new vector, scalar, and tensor interactions, denoted by $V_{L,R}$, $S_{L,R}$, and T_L, involve left-handed neutrinos, whereas the NP couplings denoted by $\tilde{V}_{L,R}$, $\tilde{S}_{L,R}$, and $\tilde{T}_L$ involve right-handed neutrinos. We consider NP contributions coming from vector- and scalar-type interactions only. We neglect the contributions coming from NP couplings that involves right-handed neutrinos, i.e., $\tilde{V}_{L,R} = \tilde{S}_{L,R} = \tilde{T}_L = 0$. All the NP couplings are assumed to be real for our analysis. With these assumptions and retaining the same notation as in Ref. [19], we obtain

$$\begin{aligned}\mathcal{L}_{\rm eff} = -\frac{G_F}{\sqrt{2}} V_{q'b}\{&G_V\bar{l}\gamma_\mu(1-\gamma_5)\nu_l\bar{q'}\gamma^\mu b \\ &- G_A\bar{l}\gamma_\mu(1-\gamma_5)\nu_l\bar{q'}\gamma^\mu\gamma_5 b \\ &+ G_S\bar{l}(1-\gamma_5)\nu_l\bar{q'} b - G_P\bar{l}(1-\gamma_5)\nu_l\bar{q'}\gamma_5 b\} \\ &+ \text{H.c.},\end{aligned} \tag{4}$$

where

$$G_V = 1 + V_L + V_R, \qquad G_A = 1 + V_L - V_R,$$
$$G_S = S_L + S_R, \qquad G_P = S_L - S_R.$$

The SM contribution can be obtained once we set $V_{L,R} = S_{L,R} = 0$ in Eq. (4).

In order to compute the branching fractions and other observables for $\Lambda_b \to \Lambda_c l\nu$ and $\Lambda_b \to p l\nu$ decay modes, we need to find various hadronic form factors that parametrizes the hadronic matrix elements of vector (axial vector) and scalar (pseudoscalar) currents between the two spin half baryons. The hadronic matrix elements of vector and axial vector currents between two spin half baryons B_1 and B_2 can be parametrized in terms of various form factors as

$$M_\mu^V = \langle B_2, \lambda_2 | J_\mu^V | B_1, \lambda_1 \rangle = \bar{u}_2(p_2, \lambda_2)[f_1(q^2)\gamma_\mu + i f_2(q^2)\sigma_{\mu\nu}q^\nu + f_3(q^2)q_\mu]u_1(p_1, \lambda_1),$$
$$M_\mu^A = \langle B_2, \lambda_2 | J_\mu^A | B_1, \lambda_1 \rangle = \bar{u}_2(p_2, \lambda_2)[g_1(q^2)\gamma_\mu + i g_2(q^2)\sigma_{\mu\nu}q^\nu + g_3(q^2)q_\mu]\gamma_5 u_1(p_1, \lambda_1), \quad (5)$$

where $q^\mu = (p_1 - p_2)^\mu$ is the four-momentum transfer, λ_1 and λ_2 are the helicities of the parent and daughter baryons, respectively and $\sigma_{\mu\nu} = \frac{i}{2}[\gamma_\mu, \gamma_\nu]$. Here $B_1 = \Lambda_b$ and $B_2 = (\Lambda_c, p)$, respectively. In order to find the hadronic matrix elements of scalar and pseudoscalar currents, we use the equation of motion. That is,

$$\langle B_2, \lambda_2 | \bar{q}' b | B_1, \lambda_1 \rangle = \bar{u}_2(p_2, \lambda_2)\left[f_1(q^2)\frac{\not{q}}{m_b - m_{q'}} + f_3(q^2)\frac{q^2}{m_b - m_{q'}}\right]u_1(p_1, \lambda_1),$$
$$\langle B_2, \lambda_2 | \bar{q}' \gamma_5 b | B_1, \lambda_1 \rangle = \bar{u}_2(p_2, \lambda_2)\left[-g_1(q^2)\frac{\not{q}}{m_b + m_{q'}} - g_3(q^2)\frac{q^2}{m_b + m_{q'}}\right]\gamma_5 u_1(p_1, \lambda_1), \quad (6)$$

where m_b is the mass of b quark and $m_{q'}$ is the mass of $q' = (u, c)$ quarks evaluated at the renormalization scale $\mu = m_b$, respectively. The various form factors f_i's and g_i's are related to the helicity form factors $f_{+,\perp,0}$ and $g_{+,\perp,0}$ as follows [60]:

$$f_+(q^2) = f_1(q^2) - \frac{q^2}{m_{B_1} + m_{B_2}} f_2(q^2),$$
$$f_\perp(q^2) = f_1(q^2) - (m_{B_1} + m_{B_2}) f_2(q^2),$$
$$f_0(q^2) = f_1(q^2) + \frac{q^2}{m_{B_1} - m_{B_2}} f_3(q^2),$$
$$g_+(q^2) = g_1(q^2) + \frac{q^2}{m_{B_1} - m_{B_2}} g_2(q^2),$$
$$g_\perp(q^2) = g_1(q^2) + (m_{B_1} - m_{B_2}) g_2(q^2),$$
$$g_0(q^2) = g_1(q^2) + \frac{q^2}{m_{B_1} + m_{B_2}} g_3(q^2), \quad (7)$$

where m_{B_1} and m_{B_2} are the masses of B_1 and B_2 baryons, respectively. For the various helicity form factors, we have used the formula given in Ref. [60]. The relevant equations pertinent for our calculation are as follows:

$$f(q^2) = \frac{1}{1 - q^2/(m_{\rm pole}^f)^2}[a_0^f + a_1^f z(q^2)], \quad (8)$$

where $m_{\rm pole}^f$ is the pole mass. Here f represents $f_{+,\perp,0}$ and $g_{+,\perp,0}$, respectively. The numerical values of $m_{\rm pole}^f$, a_0^f, and a_1^f relevant for our calculation are taken from Ref. [60]. The expansion parameter z is defined as

$$z(q^2) = \frac{\sqrt{t_+ - q^2} - \sqrt{t_+ - t_0}}{\sqrt{t_+ - q^2} + \sqrt{t_+ - t_0}}, \quad (9)$$

where $t_+ = (m_{B_1} + m_{B_2})^2$ and $t_0 = (m_{B_1} - m_{B_2})^2$, respectively. For more details, we refer to Ref. [60]. We now proceed to discuss the helicity amplitudes for these baryonic $b \to (c, u) l\nu$ decay modes. The helicity amplitudes can be defined by [59,61,64]

$$H_{\lambda_2\lambda_W}^{V/A} = M_\mu^{V/A}(\lambda_2)\epsilon^{\dagger\mu}(\lambda_W), \quad (10)$$

where λ_2 and λ_W denote the helicities of the daughter baryon and $W^-_{\text{off-shell}}$, respectively. The total left-chiral helicity amplitude can be written as

$$H_{\lambda_2\lambda_W} = H_{\lambda_2\lambda_W}^V - H_{\lambda_2\lambda_W}^A. \quad (11)$$

In terms of the various form factors and the NP couplings, the helicity amplitudes can be written as [58]

$$H_{\frac{1}{2}0}^V = G_V \frac{\sqrt{Q_-}}{\sqrt{q^2}}[(m_{B_1} + m_{B_2}) f_1(q^2) - q^2 f_2(q^2)],$$
$$H_{\frac{1}{2}0}^A = G_A \frac{\sqrt{Q_+}}{\sqrt{q^2}}[(m_{B_1} - m_{B_2}) g_1(q^2) + q^2 g_2(q^2)],$$
$$H_{\frac{1}{2}1}^V = G_V \sqrt{2Q_-}[-f_1(q^2) + (m_{B_1} + m_{B_2}) f_2(q^2)],$$
$$H_{\frac{1}{2}1}^A = G_A \sqrt{2Q_+}[-g_1(q^2) - (m_{B_1} - m_{B_2}) g_2(q^2)],$$
$$H_{\frac{1}{2}t}^V = G_V \frac{\sqrt{Q_+}}{\sqrt{q^2}}[(m_{B_1} - m_{B_2}) f_1(q^2) + q^2 f_3(q^2)],$$
$$H_{\frac{1}{2}t}^A = G_A \frac{\sqrt{Q_-}}{\sqrt{q^2}}[(m_{B_1} + m_{B_2}) g_1(q^2) - q^2 g_3(q^2)], \quad (12)$$

where $Q_\pm = (m_{B_1} \pm m_{B_2})^2 - q^2$. Either from parity or from explicit calculation, one can show that $H^V_{-\lambda_2-\lambda_W} = H^V_{\lambda_2\lambda_W}$ and $H^A_{-\lambda_2-\lambda_W} = -H^A_{\lambda_2\lambda_W}$. Similarly, the scalar and pseudoscalar helicity amplitudes associated with the NP couplings G_S and G_P can be written as [58]

$$\begin{aligned}
H^{SP}_{\frac{1}{2}0} &= H^S_{\frac{1}{2}0} - H^P_{\frac{1}{2}0},\\
H^S_{\frac{1}{2}0} &= G_S \frac{\sqrt{Q_+}}{m_b - m_{q'}}[(m_{B_1} - m_{B_2})f_1(q^2) + q^2 f_3(q^2)],\\
H^P_{\frac{1}{2}0} &= G_P \frac{\sqrt{Q_-}}{m_b + m_{q'}}[(m_{B_1} + m_{B_2})g_1(q^2) - q^2 g_3(q^2)].
\end{aligned} \tag{13}$$

Moreover, we have $H^S_{\lambda_2\lambda_{\rm NP}} = H^S_{-\lambda_2-\lambda_{\rm NP}}$ and $H^P_{\lambda_2\lambda_{\rm NP}} = -H^P_{-\lambda_2-\lambda_{\rm NP}}$ from parity argument or from explicit calculation.

We follow Ref. [58] and write the differential angular distribution for the three-body $B_1 \to B_2 l\nu$ decays in the presence of NP as

$$\begin{aligned}
\frac{d\Gamma(B_1 \to B_2 l\nu)}{dq^2 d\cos\theta_l} &= N\left(1 - \frac{m_l^2}{q^2}\right)^2\\
&\times \left[A_1 + \frac{m_l^2}{q^2}A_2 + 2A_3 + \frac{4m_l}{\sqrt{q^2}}A_4\right],
\end{aligned} \tag{14}$$

where

$$\begin{aligned}
N &= \frac{G_F^2 |V_{q'b}|^2 q^2 |\vec{p}_{B_2}|}{512\pi^3 m_{B_1}^2},\\
A_1 &= 2\sin^2\theta_l (H^2_{\frac{1}{2}0} + H^2_{-\frac{1}{2}0}) + (1-\cos\theta_l)^2 H^2_{\frac{1}{2}1} + (1+\cos\theta_l)^2 H^2_{-\frac{1}{2}-1},\\
A_2 &= 2\cos^2\theta_l (H^2_{\frac{1}{2}0} + H^2_{-\frac{1}{2}0}) + \sin^2\theta_l (H^2_{\frac{1}{2}1} + H^2_{-\frac{1}{2}-1}) + 2(H^2_{\frac{1}{2}t} + H^2_{-\frac{1}{2}t}) - 4\cos\theta_l (H_{\frac{1}{2}t}H_{\frac{1}{2}0} + H_{-\frac{1}{2}t}H_{-\frac{1}{2}0}),\\
A_3 &= (H^{SP}_{\frac{1}{2}0})^2 + (H^{SP}_{-\frac{1}{2}0})^2,\\
A_4 &= -\cos\theta_l (H_{\frac{1}{2}0}H^{SP}_{\frac{1}{2}0} + H_{-\frac{1}{2}0}H^{SP}_{-\frac{1}{2}0}) + (H_{\frac{1}{2}t}H^{SP}_{\frac{1}{2}0} + H_{-\frac{1}{2}t}H^{SP}_{-\frac{1}{2}0}).
\end{aligned} \tag{15}$$

Here $|\vec{p}_{B_2}| = \sqrt{\lambda(m_{B_1}^2, m_{B_2}^2, q^2)}/2m_{B_1}$ is the momentum of the outgoing baryon B_2, where $\lambda(a,b,c) = a^2 + b^2 + c^2 - 2(ab + bc + ca)$. We denote θ_l as the angle between the daughter baryon B_2 and the lepton three-momentum vector in the q^2 rest frame. The differential decay rate can be obtained by integrating out $\cos\theta_l$ from Eq. (14), i.e.,

$$\begin{aligned}
\frac{d\Gamma(B_1 \to B_2 l\nu)}{dq^2} &= \frac{8N}{3}\left(1 - \frac{m_l^2}{q^2}\right)^2\\
&\times \left[B_1 + \frac{m_l^2}{2q^2}B_2 + \frac{3}{2}B_3 + \frac{3m_l}{\sqrt{q^2}}B_4\right],
\end{aligned} \tag{16}$$

where

$$\begin{aligned}
B_1 &= H^2_{\frac{1}{2}0} + H^2_{-\frac{1}{2}0} + H^2_{\frac{1}{2}1} + H^2_{-\frac{1}{2}-1},\\
B_2 &= H^2_{\frac{1}{2}0} + H^2_{-\frac{1}{2}0} + H^2_{\frac{1}{2}1} + H^2_{-\frac{1}{2}-1} + 3(H^2_{\frac{1}{2}t} + H^2_{-\frac{1}{2}t}),\\
B_3 &= (H^{SP}_{\frac{1}{2}0})^2 + (H^{SP}_{-\frac{1}{2}0})^2,\\
B_4 &= H_{\frac{1}{2}t}H^{SP}_{\frac{1}{2}0} + H_{-\frac{1}{2}t}H^{SP}_{-\frac{1}{2}0}.
\end{aligned} \tag{17}$$

We define several observables such as the ratio of branching ratios R_{Λ_c}, R_p, and the ratio of partially integrated branching ratios $R^\mu_{\Lambda_c p}$ for the two decay modes such that

$$\begin{aligned}
R_{\Lambda_c} &= \frac{\mathcal{B}(\Lambda_b \to \Lambda_c \tau^- \bar{\nu}_\tau)}{\mathcal{B}(\Lambda_b \to \Lambda_c l^- \bar{\nu}_l)},\\
R_p &= \frac{\mathcal{B}(\Lambda_b \to p \tau^- \bar{\nu}_\tau)}{\mathcal{B}(\Lambda_b \to p l^- \bar{\nu}_l)},\\
R^\mu_{\Lambda_c p} &= \frac{\int_{15\ {\rm GeV}^2}^{q^2_{\rm max}} \frac{d\Gamma(\Lambda_b \to p\mu\nu)}{dq^2} dq^2}{\int_{7\ {\rm GeV}^2}^{q^2_{\rm max}} \frac{d\Gamma(\Lambda_b \to \Lambda_c \mu\nu)}{dq^2} dq^2}.
\end{aligned} \tag{18}$$

We have also defined several q^2-dependent observables such as the differential branching fractions ${\rm DBR}(q^2)$, the ratio of branching fractions $R(q^2)$, forward-backward asymmetries $A_{\rm FB}(q^2)$, and the convexity parameter $C_F^l(q^2)$ for these two baryonic decay modes. These are

$$\begin{aligned}
{\rm DBR}(q^2) &= \left(\frac{d\Gamma}{dq^2}\right)/\Gamma_{\rm tot},\\
R(q^2) &= \frac{{\rm DBR}(q^2)(B_1 \to B_2 \tau\nu)}{{\rm DBR}(q^2)(B_1 \to B_2 l\nu)},\\
A_{\rm FB}(q^2) &= \left\{\left(\int_{-1}^0 - \int_0^1\right) d\cos\theta_l \frac{d\Gamma}{dq^2 d\cos\theta_l}\right\} \Big/ \frac{d\Gamma}{dq^2},\\
C_F^l(q^2) &= \frac{1}{\mathcal{H}_{\rm tot}} \frac{d^2 W(\theta_l)}{d(\cos\theta_l)^2},
\end{aligned} \tag{19}$$

where

$$W(\theta_l) = \frac{3}{8}\left[A_1 + \frac{m_l^2}{q^2}A_2 + 2A_3 + \frac{4m_l}{\sqrt{q^2}}A_4\right],$$
$$\mathcal{H}_{\rm tot} = \int d(\cos\theta_l) W(\theta_l),$$
$$\frac{d^2W(\theta_l)}{d(\cos\theta_l)^2} = \frac{3}{4}\left(1 - \frac{m_l^2}{q^2}\right)[H^2_{\frac{1}{2}1} + H^2_{-\frac{1}{2}-1} - 2(H^2_{\frac{1}{2}0} + H^2_{-\frac{1}{2}0})]. \quad (20)$$

We want to mention that the observable $\frac{d^2W(\theta_l)}{d(\cos\theta_l)^2}$ is independent of the new scalar couplings S_L and S_R. It only depends on the new vector couplings V_L and V_R. Hence, once NP is established, this observable can be used to distinguish between the vector- and scalar-type NP interactions. We now proceed to discuss the results of our analysis.

III. RESULTS AND DISCUSSION

For definiteness, we first present all the inputs that are pertinent for our calculation. For the quark, lepton, and baryon masses, we use $m_b(m_b) = 4.18$ GeV, $m_c(m_b) = 0.91$ GeV, $m_e = 0.510998928 \times 10^{-3}$ GeV, $m_\mu = 0.1056583715$ GeV, $m_\tau = 1.77682$ GeV, $m_p = 0.938272046$ GeV, $m_{\Lambda_b} = 5.61951$ GeV, and $m_{\Lambda_c} = 2.28646$ GeV [9]. For the mean lifetime of the Λ_b baryon, we use $\tau_{\Lambda_b} = (1.466 \pm 0.010) \times 10^{-12}$ s [9]. For the CKM matrix element $|V_{cb}|$, we have used the value $|V_{cb}| = (39.5 \pm 0.8) \times 10^{-3}$ [9]. Very recently, LHCb measured the partially integrated decay rates of the Λ_b^0 baryon to decay into the $p\mu\nu$ final state relative to the $\Lambda_c^+\mu\nu$ final state to be

$$R^\mu_{\Lambda_c p} = \frac{\int_{15\ \rm GeV^2}^{q^2_{\rm max}} \frac{d\Gamma(\Lambda_b\to p\mu\nu)}{dq^2} dq^2}{\int_{7\ \rm GeV^2}^{q^2_{\rm max}} \frac{d\Gamma(\Lambda_b\to \Lambda_c\mu\nu)}{dq^2} dq^2} = (1.00 \pm 0.04 \pm 0.08) \times 10^{-2} \quad (21)$$

and put constraints on the ratio $|V_{ub}|/|V_{cb}| = 0.083 \pm 0.004 \pm 0.004$ [53]. A value of $|V_{ub}| = (32.7 \pm 2.3) \times 10^{-4}$ [53,54] is obtained using the theoretical calculations and the extracted value of $|V_{cb}|$ from exclusive B decays. This measurement of $|V_{ub}|$ using baryonic decay channel is in very good agreement with the exclusively measured world average from Ref. [52]. However, it disagrees with the inclusive measurement [9] at a significance level of 3.5σ. A very precise calculation of the $\Lambda_b \to \Lambda_c$ and $\Lambda_b \to p$ hadronic form factors using lattice QCD with $2+1$ dynamical flavors relevant for the determination of CKM elements $|V_{cb}|$ and $|V_{ub}|$ was very recently completed in Ref. [60]. The relevant parameters for the form factor calculation are given in Table I and Table II. We also report the most important experimental input parameters R_D, R_{D^*}, and R^l_π with their uncertainties in Table III. The errors in Eq. (1) are added in quadrature. Let us now proceed to discuss the results that are obtained within the SM.

The SM branching fractions and the ratio of branching fractions for the $\Lambda_b \to \Lambda_c l\nu$ and $\Lambda_b \to p l\nu$ decays are presented in Table IV. There are two main sources of uncertainties. It may arise either from not so well known input parameters such as CKM matrix elements or from hadronic input parameters such as form factors and decay constants. In order to gauge the effect of these above mentioned uncertainties on various observables, we use a random number generator and perform a random scan over all the theoretical input parameters such as CKM matrix

TABLE I. Masses (in GeV) of the relevant form factor pole taken from Ref. [60].

f	$m^f_{\rm pole}(\Lambda_b \to \Lambda_c)$	$m^f_{\rm pole}(\Lambda_b \to p)$	f	$m^f_{\rm pole}(\Lambda_b \to \Lambda_c)$	$m^f_{\rm pole}(\Lambda_b \to p)$
$f_+, f_\perp$	6.332	5.325	$g_+, g_\perp$	6.768	5.706
f_0	6.725	5.655	g_0	6.276	5.279

TABLE II. Nominal form factor parameters taken from Ref. [60].

Parameter	$\Lambda_b \to p$	$\Lambda_b \to \Lambda_c$	Parameter	$\Lambda_b \to p$	$\Lambda_b \to \Lambda_c$
$a_0^{f_+}$	0.43 ± 0.03	0.8137 ± 0.0181	$a_0^{g_+}$	0.3718 ± 0.0194	0.6876 ± 0.0084
$a_1^{f_+}$	-1.4578 ± 0.4178	-8.5673 ± 0.8444	$a_1^{g_+}$	-1.4561 ± 0.3280	-6.5556 ± 0.4713
$a_0^{f_0}$	0.3981 ± 0.0245	0.7494 ± 0.0132	$a_0^{g_0}$	0.4409 ± 0.0278	0.7446 ± 0.0156
$a_1^{f_0}$	-1.3575 ± 0.3869	-7.2530 ± 0.8114	$a_1^{g_0}$	-1.7273 ± 0.3684	-7.7216 ± 0.5437
$a_0^{f_\perp}$	0.5228 ± 0.0433	1.0809 ± 0.0262	$a_0^{g_\perp}$	0.3718 ± 0.0194	0.6876 ± 0.0084
$a_1^{f_\perp}$	-1.6943 ± 0.6834	-11.6259 ± 1.5343	$a_1^{g_\perp}$	-1.6839 ± 0.3882	-6.7870 ± 0.5013

TABLE III. Experimental input parameters.

Ratio of branching ratios:	
R_π^l	0.73 ± 0.15 [6]
R_D	0.391 ± 0.050 [52]
R_{D^*}	0.322 ± 0.022 [52]

TABLE IV. Branching ratio and ratio of branching ratios within the SM.

Observables	Central value	1σ range
$\mathcal{B}(\Lambda_b \to p l\nu)$	3.89×10^{-4}	$(1.739 - 12.870) \times 10^{-4}$
$\mathcal{B}(\Lambda_b \to p\tau\nu)$	2.75×10^{-4}	$(1.403 - 8.237) \times 10^{-4}$
$\mathcal{B}(\Lambda_b \to \Lambda_c l\nu)$	4.83×10^{-2}	$(4.316 - 5.418) \times 10^{-2}$
$\mathcal{B}(\Lambda_b \to \Lambda_c \tau\nu)$	1.63×10^{-2}	$(1.504 - 1.769) \times 10^{-2}$
R_{Λ_c}	0.3379	(0.3203–0.3559)
R_p	0.7071	(0.588–0.878)
$R^{\mu}_{\Lambda_c p}$	0.0101	(0.0043–0.0333)

elements, form factors, and decay constants within 1σ of their central values. The central values reported in Table IV are obtained using the central values of all the input parameters whereas, to find the 1σ range of all the parameters, we vary all the input parameters such as CKM matrix elements, the hadronic form factors, and the decay constants within 1σ from their central values. We, however, do not include the uncertainties coming from the quark mass, lepton mass, baryon mass, and the mean lifetime as these are not important for our analysis. Our central value for the parameter R_{Λ_c} is exactly the same as the value reported in Ref. [60]; however, it differs slightly from the values reported in Refs. [57–59]. Again, our central value of R_p reported in Table IV differs slightly from the value $R_p = 0.722$ obtained in Ref. [61]. It is expected because we have used the lattice calculations of the form factors from Ref. [60]. We, however, use only the nominal form factor parameters and their uncertainties in our analysis.

Now we proceed to discuss various NP scenarios. We want to see the effect of various NP couplings in a model-independent way. In the first scenario, we assume that NP is coming from couplings associated with new vector-type interactions, i.e., from V_L and V_R only. We vary V_L and V_R while keeping $S_{L,R} = 0$. We impose a 3σ constraint coming from the latest experimental results on R_D, R_{D^*}, and R_π^l, respectively. The allowed ranges in V_L and V_R that satisfy the 3σ experimental constraint are shown in Fig. 1. The corresponding ranges of the branching ratios and ratio of branching ratios for the $\Lambda_b \to \Lambda_c \tau\nu$ and $\Lambda_b \to p\tau\nu$ decays are as follows:

$$\begin{aligned}
\mathcal{B}(\Lambda_b \to \Lambda_c \tau\nu) &= (1.51 - 2.68) \times 10^{-2}, \\
\mathcal{B}(\Lambda_b \to p\tau\nu) &= (1.45 - 10.92) \times 10^{-4}, \\
R_{\Lambda_c} &= (0.3213 - 0.5409), \\
R_p &= (0.5746 - 1.209).
\end{aligned}$$

We see a significant deviation from the SM prediction. Depending on the NP couplings V_L and V_R, the value of branching ratios and the ratio of branching ratios can be either smaller or larger than the SM prediction. Precise measurement of $\mathcal{B}(\Lambda_b \to \Lambda_c \tau\nu)$, $\mathcal{B}(\Lambda_b \to p\tau\nu)$, R_{Λ_c}, and R_p will put additional constraints on the NP couplings V_L and V_R. We wish to look at the effect of the new physics couplings (V_L, V_R) on different observables such as the differential branching ratio $\mathrm{DBR}(q^2)$, ratio of branching ratio $R(q^2)$, forward-backward asymmetry $A_{\mathrm{FB}}(q^2)$, and the convexity parameter $C_F^l(q^2)$ for the two decay modes. In Fig. 2, we have shown in blue the allowed SM bands and in green the allowed bands of each observable once the NP couplings V_L and V_R are included. It can be seen that once NP is included the deviation from the SM expectation is quite large in case of $\mathrm{DBR}(q^2)$, $R(q^2)$, and $A_{\mathrm{FB}}(q^2)$. However, the deviation is almost negligible in case of $C_F^l(q^2)$. Again, the deviation is more in case of $\Lambda_b \to \Lambda_c \tau\nu$ decays compared to that of $\Lambda_b \to p\tau\nu$ decays.

In the second scenario, we assume that NP is coming from new scalar-type interactions, i.e., from S_L and S_R only. To explore the effect of NP coming from S_L and S_R, we vary S_L and S_R and impose a 3σ constraint coming from the

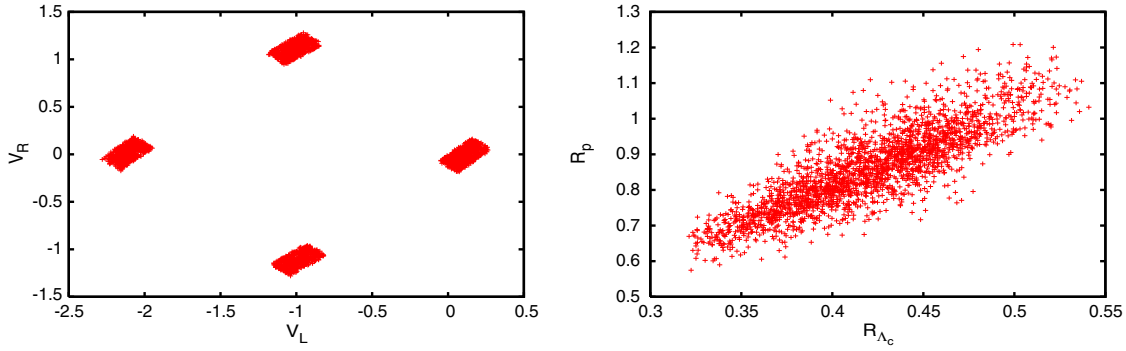

FIG. 1. Allowed regions of V_L and V_R obtained using the 3σ constraint coming from R_D, R_{D^*}, and R_π^l are shown in the left panel and the corresponding ranges in R_p and R_{Λ_c} in the presence of these NP couplings are shown in the right panel.

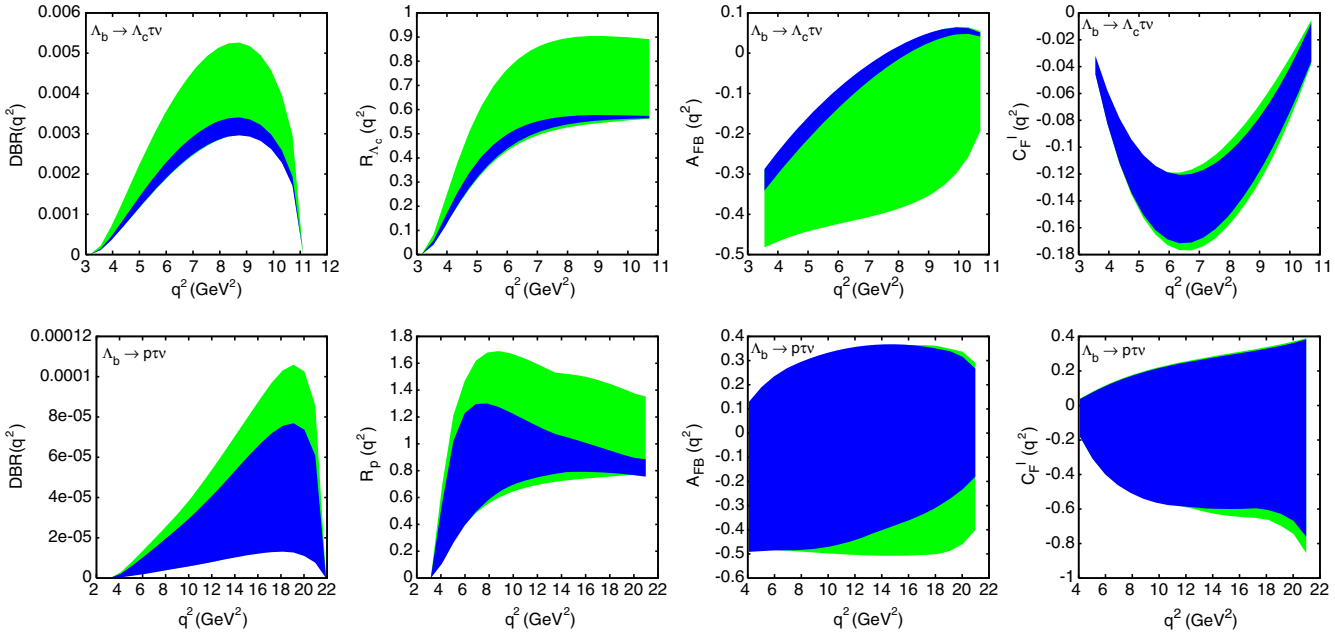

FIG. 2. The dependence of the observables DBR(q^2), $R(q^2)$, $A_{FB}(q^2)$, and $C_F^l(q^2)$ on V_L and V_R. The allowed range in each observable is shown in light (green) band once the NP couplings (V_L, V_R) are varied within the allowed ranges of the left panel of Fig. 1. The corresponding SM prediction is shown in dark (blue) band. Upper and lower panel correspond to $\Lambda_b \to \Lambda_c\tau\nu$ and $\Lambda_b \to p\tau\nu$ decay modes, respectively.

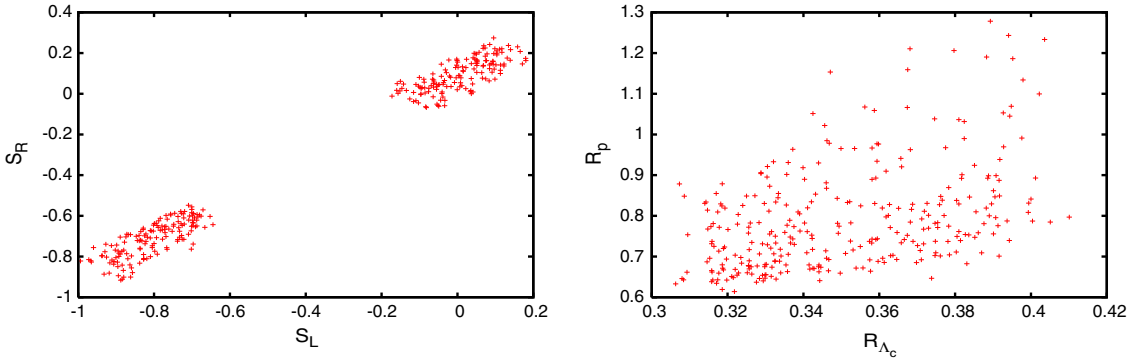

FIG. 3. Allowed regions of S_L and S_R, obtained using the 3σ constraint, coming from R_D, R_{D^*}, and R_π^l are shown in the left panel and the corresponding ranges in R_p and R_{Λ_c} in the presence of these NP couplings are shown in the right panel.

recent measurement of R_D, R_{D^*}, and R_π^l. The resulting ranges in S_L and S_R, obtained using the 3σ experimental constraint, are shown in Fig. 3. In the left panel of Fig. 3, the possible ranges in R_{Λ_c} and R_p are shown. The allowed ranges in all the observables are

$$\begin{aligned}\mathcal{B}(\Lambda_b \to \Lambda_c\tau\nu) &= (1.43 - 2.06) \times 10^{-2},\\ \mathcal{B}(\Lambda_b \to p\tau\nu) &= (1.60 - 7.85) \times 10^{-4},\\ R_{\Lambda_c} &= (0.3063 - 0.4101),\\ R_p &= (0.6139 - 1.278).\end{aligned}$$

Note that the deviation from the SM prediction can be significant depending on the values of the NP couplings S_L and S_R. We want to see the effect of these NP couplings on various q^2-dependent observables. In Fig. 4, we have shown how the observables DBR(q^2), $R(q^2)$, $A_{\rm FB}(q^2)$, and $C_F^l(q^2)$ behave as a function of q^2 with and without the NP couplings. The blue band corresponds to the SM range whereas, the green band corresponds to the NP range. The deviations from the SM expectation is prominent in case of observables such as the differential branching fraction DBR(q^2), ratio of branching fraction $R(q^2)$, and the forward-backward asymmetry parameter $A_{\rm FB}(q^2)$. However, in case of the convexity parameter $C_F^l(q^2)$, the deviation is small; almost negligible for $\Lambda_b \to p\tau\nu$ decay mode. Again, it can be seen that the deviation is more pronounced in case of $\Lambda_b \to \Lambda_c\tau\nu$ decays compared to $\Lambda_b \to p\tau\nu$ decays.

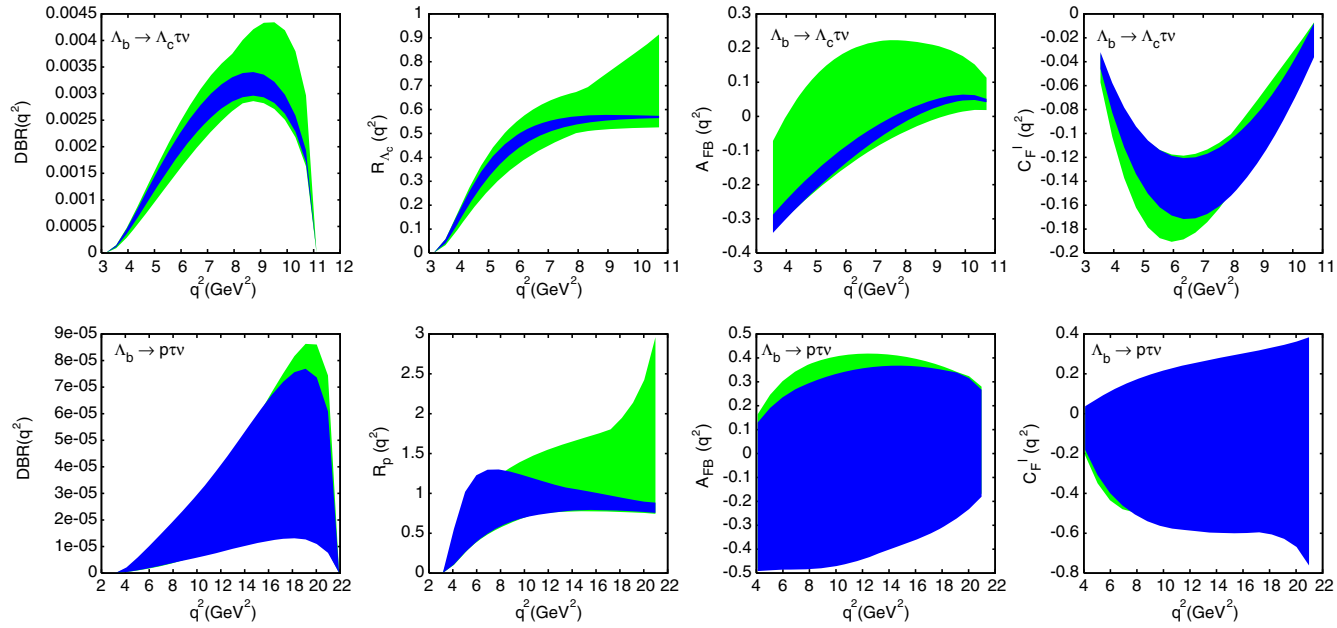

FIG. 4. The dependence of the observables DBR(q^2), $R(q^2)$, $A_{FB}(q^2)$, and $C_F^l(q^2)$ on S_L and S_R. The allowed range in each observable is shown in light (green) band once the NP couplings (S_L, S_R) are varied within the allowed ranges as shown in the left panel of Fig. 3. The corresponding SM prediction is shown in dark (blue) band. Upper and lower panel correspond to $\Lambda_b \to \Lambda_c \tau\nu$ and $\Lambda_b \to p\tau\nu$ decay modes, respectively.

We want to mention that we do not consider the pure G_V, G_A, G_S, or G_P type of NP couplings in our analysis as this kind of NP will not be able to accommodate all the existing data on R_D, R_{D^*}, and R_π^l simultaneously.

IV. CONCLUSION

Lepton flavor universality violation has been observed in various semileptonic B meson decays and, if it persists, would be a definite hint of beyond-the-SM physics. Tensions between SM prediction and experiments exist in various B meson decays to $\tau\nu$ final states mediated via $b \to u$ and $b \to c$ charged current interactions such as $B \to \tau\nu$, $B \to D\tau\nu$, and $B \to D^*\tau\nu$ decays. Similar tensions have been observed in rare B meson decays mediated via $b \to s l^+ l^-$ transition processes as well. Recent measurement of the ratio $R_K^{\mu e}$ differs from SM expectation at more than 2.5σ. Again, several interesting tensions between the experimental results and SM prediction have been observed in rare decays such as $B \to K^* \mu^+ \mu^-$ and $B \to \phi\mu^+\mu^-$ decays. Various model-dependent as well as model-independent analyses have been performed in order to explain these discrepancies. Study of $\Lambda_b \to \Lambda_c \tau\nu$ and $\Lambda_b \to p\tau\nu$ decays is important mainly for two reasons. First, these decay modes are complimentary to $B \to \tau\nu$, $B \to (D, D^*)\tau\nu$ decays mediated via $b \to c$ and $b \to u$ charged current interactions and, in principle, can provide new insights into the R_D, R_{D^*}, and R_π^l puzzle. Second, precise determination of the branching fractions of these two decay modes will be useful in determining the not so well known CKM matrix elements $|V_{ub}|$ and $|V_{cb}|$.

We study $\Lambda_b \to \Lambda_c l\nu$ and $\Lambda_b \to p l\nu$ decays mediated via $b \to u$ and $b \to c$ transitions within the context of an effective Lagrangian in the presence of NP. Similar approach was also adopted in Ref. [58]. However, in our work, we consider both $\Lambda_b \to \Lambda_c l\nu$, and $\Lambda_b \to p l\nu$ decays, mediated via $b \to u$ and $b \to c$ charged current interactions, within one framework and perform a combined analysis using the 3σ constraint coming from the most recent experimental results on R_D, R_{D^*}, and R_π^l to explore the pattern of NP. This is where we differ significantly from Ref. [58]. Moreover, the various $\Lambda_b \to \Lambda_c$ and $\Lambda_b \to p$ transition form factors that we use are also different from Ref. [58]. We assume NP in the third-generation leptons only. We also assume the NP couplings to be real for our analysis. We look at two different NP scenarios. Now let us summarize our main results.

We first report the central values and the 1σ ranges in the branching fractions, the ratio of branching fractions, and the ratio of partially integrated decay rates of $\Lambda_b \to \Lambda_c l\nu$ and $\Lambda_b \to p l\nu$ decay modes within the SM. Our value of R_{Λ_c} is exactly same as in Ref. [60], however, it differs slightly from the value reported in Refs. [57–59]. Again, our value of R_p differs slightly from the value reported in Ref. [61]. It is due to the fact that we use the latest lattice calculations of the form factors from Ref. [60].

We include vector- and scalar-type NP interactions in our analysis and explore two different NP scenarios. In the first scenario, we consider only vector-type NP interactions; i.e., we consider that only V_L and V_R contribute to these two decays modes. We find the possible ranges in V_L and V_R

using the 3σ constraint coming from the most recent experimental results on R_D, R_{D^*}, and R_π^l. The range in R_{Λ_c} and R_p with these NP couplings are found to be [0.3213, 0.5409] and [0.5746, 1.209], respectively. We also study the dependence of various q^2-dependent observables such as $\mathrm{DBR}(q^2)$, $R(q^2)$, $A_{\mathrm{FB}}(q^2)$, and $C_F^l(q^2)$ on the NP parameters V_L and V_R. We find significant deviations from the SM prediction once the NP couplings are included. However, the deviation from the SM prediction is more pronounced in the case of the $\Lambda_b \to \Lambda_c\tau\nu$ decay mode.

In the second NP scenario, we assume that NP is coming only from scalar-type interactions, i.e., from S_L and S_R only. We use the 3σ experimental constraint coming from the recent measurement of R_D, R_{D^*}, and R_π^l to find the allowed ranges in S_L and S_R. The range in R_{Λ_c} and R_p with these NP couplings are found to be [0.3063, 0.4101] and [0.6139, 1.278], respectively. It is noted that the parameter space is somewhat more constrained in this scenario. Again, for the q^2-dependent observables, we see significant deviations from the SM predictions in all the observables. Similar to the first scenario, we see that the deviation from the SM prediction is more pronounced in case of $\Lambda_b \to \Lambda_c\tau\nu$ decay mode.

Although, there is hint of NP in various leptonic and semileptonic B decays, NP is not yet established. Reduced theoretical uncertainties in the hadronic form factors, decay constants, and the CKM matrix elements will certainly help in disentangling the NP from the SM uncertainties. Again, more precise measurements are also needed to confirm the presence of NP. Measurement of all the observables for the $\Lambda_b \to \Lambda_c\tau\nu$ and $\Lambda_b \to p\tau\nu$ decay modes will be crucial to test for various NP patterns. At the same time, precise determination of the $\Lambda_b \to \Lambda_c$ and $\Lambda_b \to p$ transition form factors will also help in determining the poorly known CKM matrix element $|V_{ub}|$.

[1] R. Aaij *et al.* (LHCb Collaboration), Phys. Rev. Lett. **113**, 151601 (2014).
[2] J. P. Lees *et al.* (*BABAR* Collaboration), Phys. Rev. Lett. **109**, 101802 (2012).
[3] J. P. Lees *et al.* (*BABAR* Collaboration), Phys. Rev. D **88**, 072012 (2013).
[4] M. Huschle *et al.* (Belle Collaboration), Phys. Rev. D **92**, 072014 (2015).
[5] R. Aaij *et al.* (LHCb Collaboration), Phys. Rev. Lett. **115**, 111803 (2015); **115**, 159901 (2015).
[6] S. Fajfer, J. F. Kamenik, I. Nisandzic., and J. Zupan, Phys. Rev. Lett. **109**, 161801 (2012).
[7] I. Adachi *et al.* (Belle Collaboration), Phys. Rev. Lett. **110**, 131801 (2013).
[8] J. P. Lees *et al.* (*BABAR* Collaboration), Phys. Rev. D **88**, 031102 (2013).
[9] K. A. Olive *et al.* (Particle Data Group), Chin. Phys. C **38**, 090001 (2014).
[10] J. Charles, O. Deschamps, S. Descotes-Genon, R. Itoh, H. Lacker, A. Menzel, S. Monteil, V. Niess *et al.*, Phys. Rev. D **84**, 033005 (2011).
[11] J. Charles, A. Höcker, H. Lacker, S. Laplace, F. R. Diberder, J. Malclés, J. Ocariz, M. Pivk, and L. Roos (CKMfitter Group Collaboration), Eur. Phys. J. C **41**, 1 (2005).
[12] M. Bona *et al.* (UTfit Collaboration), Phys. Lett. B **687**, 61 (2010).
[13] A. Abdesselam *et al.* (Belle Collaboration), arXiv: 1409.5269.
[14] P. del Amo Sanchez *et al.* (*BABAR* Collaboration), Phys. Rev. D **83**, 032007 (2011).
[15] H. Ha *et al.* (Belle Collaboration), Phys. Rev. D **83**, 071101 (2011).
[16] D. Asner *et al.* (Heavy Flavor Averaging Group Collaboration), arXiv:1010.1589.
[17] P. Hamer *et al.* (Belle Collaboration), arXiv:1509.06521.
[18] D. Du, A. X. El-Khadra, S. Gottlieb, A. S. Kronfeld, J. Laiho, E. Lunghi, R. S. Van de Water, and R. Zhou, arXiv:1510.02349.
[19] R. Dutta, A. Bhol, and A. K. Giri, Phys. Rev. D **88**, 114023 (2013).
[20] F. U. Bernlochner, arXiv:1509.06938.
[21] C. H. Chen and C. Q. Geng, J. High Energy Phys. 10 (2006) 053.
[22] A. Khodjamirian, T. Mannel, N. Offen, and Y.-M. Wang, Phys. Rev. D **83**, 094031 (2011).
[23] P. Krawczyk and S. Pokorski, Phys. Rev. Lett. **60**, 182 (1988).
[24] J. Kalinowski, Phys. Lett. B **245**, 201 (1990).
[25] W. S. Hou, Phys. Rev. D **48**, 2342 (1993).
[26] M. Tanaka, Z. Phys. C **67**, 321 (1995).
[27] J. F. Kamenik and F. Mescia, Phys. Rev. D **78**, 014003 (2008).
[28] U. Nierste, S. Trine, and S. Westhoff, Phys. Rev. D **78**, 015006 (2008).
[29] M. Tanaka and R. Watanabe, Phys. Rev. D **82**, 034027 (2010).
[30] S. Fajfer, J. F. Kamenik, and I. Nisandzic, Phys. Rev. D **85**, 094025 (2012).
[31] Y. Sakaki and H. Tanaka, Phys. Rev. D **87**, 054002 (2013).
[32] A. Datta, M. Duraisamy, and D. Ghosh, Phys. Rev. D **86**, 034027 (2012).
[33] A. Soffer, Mod. Phys. Lett. A **29**, 1430007 (2014).
[34] J. A. Bailey *et al.*, Phys. Rev. Lett. **109**, 071802 (2012).
[35] D. Bečirević, N. Košnik, and A. Tayduganov, Phys. Lett. B **716**, 208 (2012).
[36] M. Tanaka and R. Watanabe, Phys. Rev. D **87**, 034028 (2013).

[37] M. Freytsis, Z. Ligeti, and J. T. Ruderman, Phys. Rev. D **92**, 054018 (2015).
[38] S. Bhattacharya, S. Nandi, and S. K. Patra, arXiv: 1509.07259.
[39] A. Celis, M. Jung, X. Q. Li, and A. Pich, J. High Energy Phys. 01 (2013) 054.
[40] P. Ko, Y. Omura, and C. Yu, J. High Energy Phys. 03 (2013) 151.
[41] A. Crivellin, C. Greub, and A. Kokulu, Phys. Rev. D **86**, 054014 (2012).
[42] N. G. Deshpande and A. Menon, J. High Energy Phys. 01 (2013) 025.
[43] Y. Sakaki, M. Tanaka, A. Tayduganov, and R. Watanabe, Phys. Rev. D **88**, 094012 (2013).
[44] A. Greljo, G. Isidori, and D. Marzocca, J. High Energy Phys. 07 (2015) 142.
[45] I. Doršner, S. Fajfer, N. Košnik, and I. Nišandžić, J. High Energy Phys. 11 (2013) 084.
[46] P. Biancofiore, P. Colangelo, and F. De Fazio, Phys. Rev. D **87**, 074010 (2013).
[47] Y. Y. Fan, Z. J. Xiao, R. M. Wang, and B. Z. Li, arXiv: 1505.07169.
[48] C. Hati, G. Kumar, and N. Mahajan, arXiv:1511.03290.
[49] S. L. Glashow, D. Guadagnoli, and K. Lane, Phys. Rev. Lett. **114**, 091801 (2015).
[50] B. Bhattacharya, A. Datta, D. London, and S. Shivashankara, Phys. Lett. B **742**, 370 (2015).
[51] A. Hicheur, arXiv:1509.07708.
[52] Y. Amhis *et al.* (Heavy Flavor Averaging Group (HFAG) Collaboration), arXiv:1412.7515.
[53] R. Aaij *et al.* (LHCb Collaboration), Nat. Phys. **11**, 743 (2015).
[54] M. Fiore, arXiv:1511.00105.
[55] R. Aaij *et al.* (LHCb Collaboration), Phys. Rev. D **85**, 032008 (2012).
[56] R. Aaij *et al.* (LHCb Collaboration), J. High Energy Phys. 08 (2014) 143.
[57] R. M. Woloshyn, Proc. Sci. Hadron **2013**, 203 (2013).
[58] S. Shivashankara, W. Wu, and A. Datta, Phys. Rev. D **91**, 115003 (2015).
[59] T. Gutsche, M. A. Ivanov, J. G. Körner, V. E. Lyubovitskij, P. Santorelli, and N. Habyl, Phys. Rev. D **91**, 074001 (2015); **91**, 119907 (2015).
[60] W. Detmold, C. Lehner, and S. Meinel, Phys. Rev. D **92**, 034503 (2015).
[61] T. Gutsche, M. A. Ivanov, J. G. Körner, V. E. Lyubovitskij, and P. Santorelli, Phys. Rev. D **90**, 114033 (2014).
[62] T. Bhattacharya, V. Cirigliano, S. D. Cohen, A. Filipuzzi, M. Gonzalez-Alonso, M. L. Graesser, R. Gupta, and H.-W. Lin, Phys. Rev. D **85**, 054512 (2012).
[63] V. Cirigliano, J. Jenkins, and M. Gonzalez-Alonso, Nucl. Phys. **B830**, 95 (2010).
[64] J. G. Korner and G. A. Schuler, Z. Phys. C **46**, 93 (1990).